Determination of quadrupolar and chemical shielding tensors using solid-state two-dimensional NMR spectroscopy

J. S. Shore[a] and S. H. Wang
Materials Science Division, Lawrence Berkeley Laboratory and Department of Chemistry, University of California, Berkeley, California 94720

R. E. Taylor
Chemical Sciences Division, Lawrence Berkeley Laboratory and Department of Chemical Engineering, University of California, Berkeley, California 94720

A. T. Bell
Materials Science Division, Lawrence Berkeley Laboratory and Department of Chemical Engineering, University of California, Berkeley, California 94720

A. Pines[b]
Materials Science Division, Lawrence Berkeley Laboratory and Department of Chemistry, University of California, Berkeley, California 94720

(Received 7 August 1995; accepted 30 July 1996)

The quadrupolar and chemical shift tensors, as well as the relative orientation of the two principle axis systems, are accurately determined using a two-dimensional nuclear magnetic resonance technique. Good agreement between experimental and simulated two-dimensional spectra is obtained for a series of rubidium and sodium compounds at multiple magnetic field strengths. Extension of this technique to correlate the quadrupolar and dipolar interactions, as well as the incorporation of a purely isotropic dimension resulting in a three-dimensional experiment is also discussed. © *1996 American Institute of Physics.* [S0021-9606(96)02241-6]

INTRODUCTION

Nuclear magnetic resonance (NMR) spectroscopy is ideally suited for the study of the atomic, magnetic, and electronic structures of materials because it is atomic-site specific and able to provide atomic level information. While there have been many NMR experiments developed and implemented for spin-half nuclei ($I=1/2$), NMR spectroscopy of quadrupolar nuclei ($I>1/2$) has been underutilized due to a lack of sophisticated experiments that are able to exploit the quadrupolar interaction to provide useful structural and chemical information. The recent development of dynamic-angle spinning (DAS), double rotation (DOR), and multiple-quantum experiments have made it possible to obtain high resolution spectra of quadrupolar nuclei.[1–3] However, techniques to deconvolute the surfeit of information present in the NMR spectra of quadrupolar nuclei are still needed.

Approximately 60% of the NMR-active isotopes are quadrupolar, including ^{6,7}Li, ^{10,11}B, ^{17}O, ^{23}Na, ^{27}Al, ^{51}V, ^{63,65}Cu, ^{69,71}Ga, and ^{85,87}Rb. Quadrupolar nuclei are affected by the magnetic interactions experienced by spin one-half nuclei, such as the chemical shift and dipolar interactions, in addition to an electrostatic interaction between the quadrupolar moment of the nucleus and the surrounding electric field gradient (efg). Both the quadrupolar and chemical shift interactions have anisotropic contributions that are dependent on the orientation of the molecular frame relative to the magnetic field and are most conveniently characterized in a principle axis system (PAS) defined relative to the molecular frame. In the corresponding principle axis systems, three parameters are sufficient to characterize the chemical shift interaction (the isotropic shift $\delta_{\rm iso}$, the anisotropic shift δ, and the asymmetry parameter $\eta_{\rm CS}$), and two parameters are sufficient to describe the quadrupolar interaction (the quadrupolar coupling constant C_Q, and the asymmetry parameter η_Q). Unlike the chemical shift, the quadrupolar interaction is traceless, and accordingly there is no quadrupolar parameter analogous to the isotropic chemical shift.

The magnitudes and symmetries of the quadrupolar and chemical shift interactions can potentially be determined from NMR spectra and used to characterize the local atomic environment. For example, the isotropic chemical shift has been used as an analytical tool for identifying chemical species in both solutions and solids. The anisotropic chemical shift, which is more sensitive to the local atomic environment is also beginning to be used as an analytical tool. Furthermore, several groups are using the orientation-dependent nature of the chemical shift anisotropy to study molecular dynamics in many materials. The quadrupolar interaction is very sensitive to the details of bonding and for example has been used to measure the distribution of Si–O–Si bond angles in silicate glasses.[4,5]

Due to the anisotropic contributions of the quadrupolar and chemical shift interactions and the random orientations of crystallites present in powder samples, NMR spectra of powders have typically low resolution. When there are no overlapping resonances and one interaction clearly dominates the NMR line shape, the quadrupolar or chemical shift

[a]Present address: Department of Chemistry and Biochemistry, South Dakota State University, Brookings, SD 57007.
[b]Author to whom correspondence should be addressed at the University of California.

parameters can easily be determined.[6] However, the presence of overlapping resonances or of multiple interactions often precludes accurate interpretation of one-dimensional NMR spectra.

For spin one-half nuclei, spinning a powder sample about 54.74° (the ''magic'' angle) relative to the magnetic field orientationally averages the anisotropic contributions of the chemical shift and dipolar interactions, resulting in high-resolution NMR spectra.[7–9] This technique is referred to as magic-angle spinning (MAS). The anisotropic contribution of the quadrupolar interaction can be averaged by spinning the sample about two angles relative to the magnetic field either simultaneously or sequentially, as in double rotation (DOR) or dynamic angle spinning (DAS), respectively.[1,2] Isotropic spectra of quadrupolar nuclei can also be obtained by spinning the sample at one angle and exciting a multiple-quantum transition.[3] When the quadrupolar interaction is the dominant interaction and there are no overlapping resonances, simulations of MAS NMR spectra typically yield more accurate values of the quadrupolar parameters than those obtained from static powder samples, due to the removal of the line-broadening effects of the chemical shift and dipolar interactions. When the chemical shift anisotropy and dipolar interactions are negligible, spinning the sample between 60° and 70° relative to the magnetic field, yields the highest resolution of any single-quantum, single-angle spinning experiment.[10,11]

The quadrupolar and chemical shift interactions are characterized by two and three parameters, respectively. When both interactions are simultaneously present, the three angles that describe the relative orientation of the two principal axis systems are needed to completely characterize the local atomic environment and to simulate the NMR spectrum. Only recently have noncoincident principle axis systems been considered and attempts at determining all eight parameters by fitting one-dimensional NMR spectra been made.[12–20] For example, Cheng *et al.* reported values for all eight parameters for a series of rubidium salts from the fitting of ^{85}Rb and ^{87}Rb static NMR spectra.[13] These rubidium isotopes have substantially different nuclear magnetic and nuclear quadrupolar moments, enabling the determination of the quadrupolar and chemical shift interaction parameters from NMR spectra of static powder samples. However, most elements do not have two convenient NMR-active isotopes, thus precluding the general use of this method. Jakobsen *et al.* observed all the NMR transitions of ^{51}V using MAS and were able to determine all eight parameters from a comparison with simulations.[20] However, this technique is limited to quadrupolar coupling constants (C_Q) typically smaller than 2.5 MHz. The disadvantages of these one-dimensional NMR methods also include the difficulty of accurately measuring the entire NMR line shape over the typically broad spectral range and of determining a unique set of parameters to fit the NMR spectra.

Two-dimensional NMR spectroscopy has been used to accurately characterize multiple interactions. For example, separated local field spectroscopy has been used to measure the strengths and relative orientation of the dipolar and chemical shift interactions.[21–23] In this paper, the application of a two-dimensional NMR technique to determine the strengths and symmetries of the quadrupolar and chemical shift interactions, as well as the relative orientation of the principle axis systems is demonstrated. This technique has the advantages of not depending as strongly on intensity measurements as the one-dimensional methods and of being suitable for coupling constants (C_Q) between roughly 3 and 15 MHz, depending on nuclear spin quantum number, spinning speed, and field strength. Also, the technique and formalism presented in this paper can be adopted to correlate the quadrupolar and dipolar interactions; extension to a three-dimensional experiment incorporating a purely isotropic dimension for the study of systems with overlapping resonances or with a distribution of isotropic shifts such as glasses, is also possible.

EXPERIMENT

All samples used in this study were obtained from commercial sources, typically with a stated purity of 99.8%. The ^{23}Na and ^{87}Rb NMR spectra were acquired at 4.2 T (^{23}Na, 49.1 MHz; ^{87}Rb 60.8 MHz), 9.4 T (^{23}Na, 105.9 MHz; ^{87}Rb 130.9 MHz) or 11.7 T (^{23}Na, 132.3 MHz; ^{87}Rb 163.6 MHz), with a Nalorac Quest, Bruker AM-400 or a Chemagnetics CMX-500 spectrometer, respectively. A home-built NMR probe based on the design of Eastman *et al.*[24] capable of fast reorientation of the spinning axis, and employing a Doty Scientific (Columbia, SC) 5 mm fast MAS stator was used; except for the ^{23}Na NMR spectra acquired at 4.2 T, for which a probe based on the design of Mueller *et al.*[25] was used. A Whedco (Ann Arbor, MI) high torque stepping motor and motor controller were used to reorient the rotor axis in typically 40 ms. The spinning axis was initially set to 54.74° using the ^{81}Br NMR signal of KBr. To obtain pure phase two-dimensional NMR spectra, standard pulse sequences using TPPI[26] (at 9.4 T) or the method of States *et al.*[27] (at 4.2 and 11.7 T) were used. When necessary because of broad spectral ranges, an echo synchronized to the spinning of the rotor was used for detection. To ensure selective excitation of the central transition, 90° rf pulses were typically longer than 10 μs. Generally, 128 and 512 points were acquired in t_1 and t_2, respectively, with 32 scans per t_1 value. However, the experimental parameters depended greatly on sample and field strength. During processing, the t_1 dimension was zero filled to 256 points and 100 Hz Gaussian line broadening was applied in both dimensions. Dilute aqueous solutions of $RbNO_3$ and NaCl were used as external standards.

The simulations were performed on a Silicon Graphics (Mountain View, CA) R4000 workstation using a program written in FORTRAN. A two-dimensional spectrum with 128 points in both dimensions takes approximately 3 s to calculate.

THEORETICAL BACKGROUND

For the measurements presented in this paper, only the central transition ($\pm 1/2$) is considered; the quadrupolar and

chemical shift interactions are treated as perturbations to the nuclear Zeeman interaction. The quadrupolar interaction is an electrostatic interaction between a nonspherical nucleus and the electric field gradient (efg) at the nucleus, the strength of which depends on the orientation of the molecular frame relative to the static magnetic field. The efg is due to the surrounding electrons and neighboring atoms. The chemical shift interaction arises from the interaction between the electrons surrounding the nucleus and the static magnetic field and also depends on the orientation of the molecular frame relative to the static magnetic field. The following derivation of the NMR frequency shift due to the quadrupolar and chemical shift interactions follows that of Baltisberger.[28]

In terms of spin operators, the quadrupolar (H_Q) and chemical shift (H_{CS}) Hamiltonians can be written as[28–30]

$$H_Q=\frac{eQ}{2\hbar I(2I-1)}\,\mathbf{I}\cdot\mathbf{V}\cdot\mathbf{I},$$
$$H_{CS}=\gamma\hbar\mathbf{I}\cdot\boldsymbol{\sigma}\cdot\mathbf{B}, \tag{1}$$

where $\mathbf{I}$ is the nuclear spin operator and I is the nuclear spin quantum number; Q is the nuclear quadrupole moment; $\mathbf{B}$ is the static magnetic field; $\mathbf{V}$ and $\boldsymbol{\sigma}$ are the efg and the chemical shielding tensors, respectively. The Hamiltonians are written as tensor products, consistent with the anisotropic nature of the interactions. In the appropriate principle axis system, the interaction tensors ($\mathbf{V}$ and $\boldsymbol{\sigma}$) can be diagonalized separately. The diagonal elements are typically defined using the following conventions;

$$|V_{zz}|\geqslant|V_{yy}|\geqslant|V_{xx}|,$$
$$|\boldsymbol{\sigma}_{zz}-\boldsymbol{\sigma}_{iso}|\geqslant|\boldsymbol{\sigma}_{yy}-\boldsymbol{\sigma}_{iso}|\geqslant|\boldsymbol{\sigma}_{xx}-\boldsymbol{\sigma}_{iso}|,$$
$$\boldsymbol{\sigma}_{iso}=\frac{\boldsymbol{\sigma}_{zz}+\boldsymbol{\sigma}_{yy}+\boldsymbol{\sigma}_{xx}}{3}. \tag{2}$$

The subscripts zz, yy, and xx indicate orthogonal axes in the relevant principle axis system. The quadrupolar interaction is traceless and can be completely characterized by two parameters, the quadrupolar coupling constant (C_Q) and the asymmetry parameter (η_Q),

$$C_Q=\frac{e^2qQ}{\hbar},\quad \eta_Q=\frac{V_{xx}-V_{yy}}{V_{zz}}, \tag{3}$$

with $eq=V_{zz}$ by definition. The chemical shift interaction, however, requires three parameters that are conveniently defined in parts per million (ppm) relative to a standard [$\delta=10^6(\sigma_{standard}-\sigma_{sample})$]. The three parameters are the isotropic chemical shift (δ_{iso}), anisotropic chemical shift (δ), and asymmetry parameter (η_{CS}), defined as

$$\delta_{iso}=\frac{\delta_{zz}+\delta_{yy}+\delta_{xx}}{3},\quad \delta=\delta_{zz}-\delta_{iso},$$
$$\eta_{CS}=\frac{\delta_{xx}-\delta_{yy}}{\delta_{zz}-\delta_{iso}},\quad |\delta_{zz}-\delta_{iso}|\geqslant|\delta_{yy}-\delta_{iso}|\geqslant|\delta_{xx}-\delta_{iso}|. \tag{4}$$

In this convention, δ can be either positive or negative, while η_{CS} is between 0.0 and 1.0.

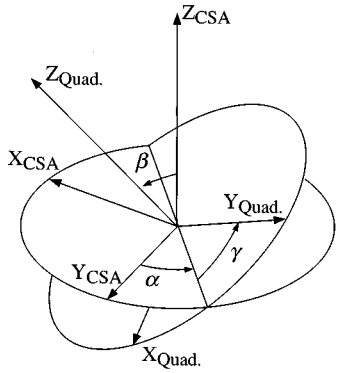

FIG. 1. A schematic representation of the quadrupolar and chemical shift principle axis systems (PAS) with a relative orientation characterized by the Euler angles α, β, and γ.

When the quadrupolar and chemical shift interactions are present simultaneously, knowledge of the relative orientation between the two interaction tensors is necessary to simulate the NMR spectrum and to completely characterize the local atomic environment. Three Euler angles (α,β,γ) can be used to characterize the relative orientation of the two principle axis systems and are defined as shown in Fig. 1. As reported by Fernandez *et al.*[18] due to the periodicity of the dependence of the quadrupolar and chemical shift interactions on the relative orientation between the molecular frame and the applied magnetic field ($\mathbf{B}$) and also the traceless nature of the quadrupolar interaction, for powders there are four distinct relative orientations of the quadrupolar and chemical shift tensors that are indistinguishable. The four orientations are related by the following symmetry operations:[18]

$$(\alpha,\beta,\gamma)\equiv(\alpha,\beta,\pi+\gamma)\equiv(\pi-\alpha,\beta,-\gamma)$$
$$\equiv(\alpha,\pi-\beta,-\gamma). \tag{5}$$

Interactions relevant to NMR are often represented by irreducible tensor operators to exploit the symmetries of the interactions and reduce the computational difficulties. The quadrupolar and chemical shift Hamiltonians, each defined in their corresponding principal axis system, can be written in terms of spherical tensors as[28–30]

$$H_{CS}^{PAS}=\hbar\gamma\delta_{iso}B_zI_z+\sqrt{\tfrac{2}{3}}\,\hbar\gamma\delta\sum_{m=-2}^{2}(-1)^m\rho_{2,-m}^{CS}T_{2,m}^{CS},$$
$$H_Q^{PAS}=\frac{\hbar C_Q}{2I(2I-1)}\sum_{m=-2}^{2}(-1)^m\rho_{2,-m}^{Q}T_{2,m}^{Q}, \tag{6}$$

where the interactions have been separated into spatial (ρ) and spin (T) components.

To calculate the NMR transition frequency, the Hamiltonians were transformed from the relevant PAS to the laboratory frame using Wigner rotation matrices. The chemical shift (CS) Hamiltonian was first transformed into the PAS of the quadrupolar interaction (QI). The quadrupolar and chemical shift Hamiltonians were then transferred to the rotor frame, and then finally to the laboratory frame

$$\text{CS PAS} \xrightarrow{(\alpha,\beta,\gamma)} \text{QI PAS} \xrightarrow{(\phi,\chi,\varphi)} \text{Rotor Frame} \xrightarrow{(\omega_r t,\theta,0)} \text{Lab Frame},$$

where (α,β,γ), (ϕ,χ,φ), $(\omega_r t,\theta,0)$ are Euler angles between the corresponding reference frames. Here ω_r is the spinning speed, and θ is the orientation of the rotor axis relative to the magnetic field. In the laboratory reference frame, the spatial parts of the quadrupolar and chemical shift interactions are[28–30]

$$\begin{aligned} A^{\mathrm{CS}}_{2,m} &= \sum_{k=-2}^{2}\sum_{l=-2}^{2}\sum_{n=-2}^{2} \rho^{\mathrm{CS}}_{2,n} D^{(2)}_{nl}(\alpha,\beta,\gamma) \\ &\quad \times D^{(2)}_{lk}(\phi,\chi,\varphi) D^{(2)}_{km}(\omega_r t,\theta,0), \\ A^{Q}_{2,m} &= \sum_{l=-2}^{2}\sum_{n=-2}^{2} \rho^{Q}_{2,n} D^{(2)}_{nl}(\phi,\chi,\varphi) D^{(2)}_{lm}(\omega_r t,\theta,0). \end{aligned} \tag{7}$$

$D^{(2)}_{ij}$ are second-rank Wigner rotation matrices.[31,32]

The NMR resonance frequency offset for a specific crystallite is a summation of the chemical shift (ω^{CS}) and quadrupolar (ω^{Q}) terms. The chemical shift contribution can be calculated using first-order perturbation theory[28]

$$\omega^{\mathrm{CS}} = \gamma B\left(\delta_{\mathrm{iso}} + \sqrt{\frac{2}{3}}\,\delta A^{\mathrm{CS}}_{2,0}\right). \tag{8}$$

Second-order perturbation theory is necessary to calculate the effect of the quadrupolar interaction on the central transition of half-integer spin nuclei[28]

$$\omega^{Q}_{1/2\rightarrow -1/2} = \frac{C_Q^2}{\gamma B[2I(2I-1)]^2}\left[I(I+1)-\frac{3}{4}\right](2A^{Q}_{21}A^{Q}_{2-1} + A^{Q}_{22}A^{Q}_{2-2}). \tag{9}$$

Notice that ω^{CS} is linearly dependent on the magnetic field strength (B) and ω^{Q} is inversely dependent on B.

It is instructive to write the dependence of ω^{CS} and ω^{Q} on θ in terms of the second and fourth order Legendre polynomials P_2 and P_4. For fast sample rotation, the time average of the frequency shift due to the chemical shift anisotropy and the second-order quadrupolar interaction are independent of the spinning speed ω_r and the angle φ,[28]

$$\begin{aligned} &\omega^{\mathrm{CS}}(\alpha,\beta,\gamma,\phi,\chi,\theta) \\ &\quad = \gamma B[\,\delta_{\mathrm{iso}} + A^{\mathrm{CS}}_2(\alpha,\beta,\gamma,\phi,\chi)P_2(\cos\,\theta)], \\ &\omega^{Q}_{1/2\rightarrow -1/2}(\phi,\chi,\theta) \\ &\quad = \omega^{2Q}_{\mathrm{iso}} + A^{Q}_2(\phi,\chi)P_2(\cos\,\theta) + A^{Q}_4(\phi,\chi)P_4(\cos\,\theta). \end{aligned} \tag{10}$$

A^{CS}_2, A^{Q}_2, and A^{Q}_4 are functions of the relative orientation for the crystallites in the rotor frame characterized by the angles ϕ and χ. A^{CS}_2 also depends on the relative orientation of the quadrupolar and chemical shift principle axis systems characterized by the angles α, β, and γ. In Fig. 2, P_2 and P_4 are shown as a function of θ. The different dependence on θ, of the chemical shift and quadrupolar interaction enables the deconvolution and measurement of the two interactions.

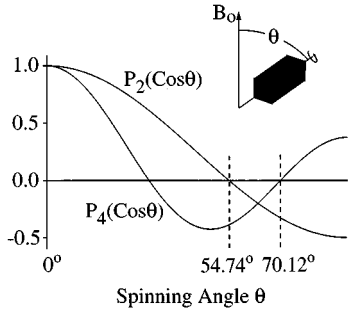

FIG. 2. The second and fourth order Legendre polynomials as a function of θ.

Also, notice that for θ equal to 54.74°, $P_2(\cos\theta)$ and hence, the anisotropic part of ω^{CS} is zero. There is no single angle for which $P_2(\cos\theta)$ and $P_4(\cos\theta)$ are simultaneously zero.

One-dimensional NMR spectra of powder samples are calculated by determining the frequency shifts for all possible crystallite orientations relative to the static magnetic field.[29,30] The frequency shift is a summation of ω^{CS} and ω^{Q} contributions. The intensity at each frequency is proportional to the population of the corresponding orientations. For a random powder sample, all orientations can be accounted for by integrating over the surface of a unit sphere. Alderman *et al.*[33] devised a computationally faster technique by approximating the surface of a unit sphere with the surface of an octahedron. The sines and cosines in the expressions of ω^{CS} and ω^{Q} can then be replaced by ratios of the coordinates on the surface of the octahedron. The simulated spectra in this paper were calculated using this method.[33]

For a powder sample the NMR frequency as a function of orientation is typically not single valued, hence for one-dimensional spectra there is overlap of signals corresponding to crystallites with different orientations, making interpretation of spectra difficult. In a two-dimensional experiment, the frequency of each nuclear spin is sampled during two different time periods. The intensity of the resulting two-dimensional spectrum is proportional to the joint probability distribution of a nuclear spin having the NMR frequency ω_1 during the first time period and ω_2 during the second time period. For the pulse sequence schematically represented in Fig. 3, the intensity of the resulting two-dimensional NMR spectrum is proportional to the probability that a nuclear spin will have a NMR frequency ω_1 for a powder sample spinning about θ_1 multiplied by the probability that the same nuclear spin will have the NMR frequency ω_2 when the sample is spinning about an axis inclined at θ_2 relative to the static magnetic field. As indicated by Eq. (10), the size of the chemical shift and quadrupolar contributions to the NMR frequency shift depends on θ. Because θ is different for each of the two dimensions, the relative contributions of the chemical shift and quadrupolar interactions will be different for the two dimensions. The resulting spectrum can be used to determine the quadrupolar and chemical shift interaction parameters, as well as the relative orientation of the principle axis systems by comparison with calculated spectra. The two-dimensional NMR spectra are calculated by determining

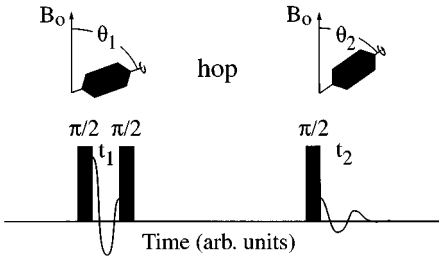

FIG. 3. A schematic representation of the switched-angle spinning (SAS) experiment. As the sample is spinning about θ_1 relative to the magnetic field, a 90° rf pulse is applied. The magnetization evolves in the plane transverse to the magnetic field for a time t_1 until another rf pulse stores the magnetization along the field axis. The spinning axis is then changed to θ_2. A final rf pulse places the magnetization back into the transverse plane where it is detected. The experiment is repeated with t_1 incremented by a dwell time.

the frequency shifts for θ_1 and θ_2, for all possible crystallite orientations. The intensity at each two-dimensional coordinate is proportional to the population of the corresponding orientation.

The experiment schematically represented in Fig. 3 was initially developed to correlate isotropic (θ_2=54.74°) and anisotropic (θ_1=90°) spectra of spin-half nuclei and is referred to as switched angle spinning (SAS).[34,35] Isotropic spectra of quadrupolar nuclei can be obtained with the same experiment if θ_1 and θ_2 are chosen such that,

$$P_2(\cos\ \theta_1) = -kP_2(\cos\ \theta_2), \tag{11}$$

$$P_4(\cos\ \theta_1) = -kP_4(\cos\ \theta_2), \tag{12}$$

where k is a constant between one and five, in which case the experiment is referred to as dynamic-angle spinning (DAS).[1,2] Although the technique introduced in this paper has similarities to both SAS and DAS, in this paper it is referred to as SAS, reserving DAS for experiments used to measure isotropic spectra of quadrupolar nuclei. SAS can also be used to correlate the dipolar and quadrupolar interactions. The dipolar interaction has the same orientation dependence as the chemical shift interaction. Also, a three-dimensional technique with a purely isotropic dimension can be developed by adding another time period at the beginning of the experiment in Fig. 3 and choosing θ_1 and θ_2 such that Eqs. (11) and (12) are satisfied. Frydman *et al.* have developed a similar technique that samples the three-dimensional space in a non-Cartesian fashion,[36,37] analogous to the two-dimensional, variable-angle correlation spectroscopy (VACSY).[38] These three-dimensional experiments will be useful for systems with multiple sites or with inhomogeneously broadened lines.

For the measurements presented in this paper, θ_2 was chosen as 54.74°, the angle at which, for fast enough spinning speeds, the anisotropic parts of both the chemical shift and dipolar interactions are effectively averaged to zero. θ_1 was chosen either to obtain the highest resolution when multiple sites were present, or for experimental ease. For example, if the inhomogeneous line-broadening is large, θ_1 equal to 90° yields a much simpler spectrum, because at this angle the odd-order spinning side-bands are not present. In Fig. 4, simulated two-dimensional SAS spectra considering only the quadrupolar interaction are shown as a function of θ_1 and the quadrupolar asymmetry parameter (η_Q). The SAS technique is very sensitive to η_Q and produces very well defined two-dimensional line shapes.

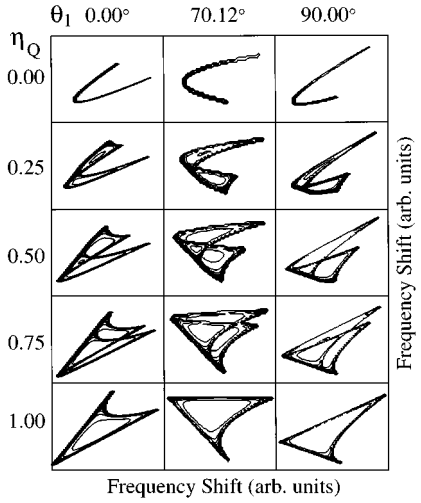

FIG. 4. Simulated two-dimensional SAS spectra, considering only the quadrupolar interaction, as a function of θ_1 and the quadrupolar asymmetry parameter, η_Q. θ_2 is 54.74°. The horizontal dimension is the ω_2 (MAS) dimension.

RESULTS AND DISCUSSION

As a test of the technique and the simulation program, a sample was chosen that had been studied previously[10,39] and contains one crystallographically distinct sodium site that has negligible chemical shift anisotropy. In Fig. 5, the experimental and simulated ^{23}Na SAS NMR spectra of Na_2SO_4 acquired with θ_1 and θ_2 equal to 80° and 54.74°, respectively, are shown. The simulated spectrum yields C_Q=2.6 MHz, η_Q=0.6, and δ_{iso}=4 ppm, consistent with previously reported values.[10,39] The projection of the ω_2 dimension (not shown) corresponds to a MAS spectrum and is consistent

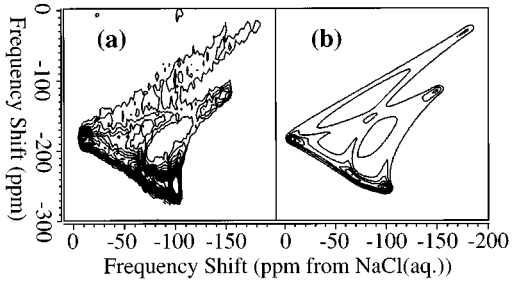

FIG. 5. (a) Experimental and (b) simulated two-dimensional ^{23}Na SAS NMR spectra of Na_2SO_4 acquired at 4.2 T with θ_1=80°, and θ_2=54.74°. The experimental spectrum was acquired with $\pi/2$ pulse lengths of 3.4 μs at both angles and a recycle delay of 2 s. The simulated spectrum corresponds to C_Q=2.6 MHz, η_Q=0.6, and δ_{iso}=4 ppm. No chemical shift anisotropy was included in the simulation. The contour levels span from 3.5% to 70% in 3.5% increments. The horizontal dimension is the ω_2 (MAS) dimension.

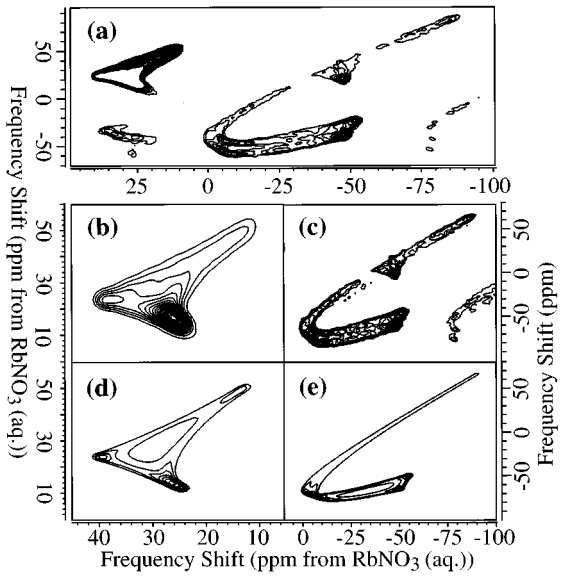

FIG. 6. Experimental and simulated two-dimensional ^{87}Rb SAS NMR spectra of Rb_2SO_4 acquired at 9.4 T with $\theta_1=90°$ and $\theta_2=54.74°$. The simulated spectra were calculated for $C_Q=5.3$ and 2.6 MHz, $\eta_Q=0.1$ and 1.0, and $\delta_{iso}=16$ and 40 ppm, respectively. The horizontal dimension is the ω_2 (MAS) dimension. (a). SAS spectrum with two sites (Contour levels: 1%–20%, 1% increments). (b) and (d): Experimental and simulated spectra for site I with $C_Q=2.6$ MHz (Contour level: 5%–100%, 5% increments). (c) and (e): Experimental (Contour levels: 0.5%–10%, 0.5% increments) and simulated (Contour levels: 5%–100%, 5% increments) spectra for site II with $C_Q=5.3$ MHz.

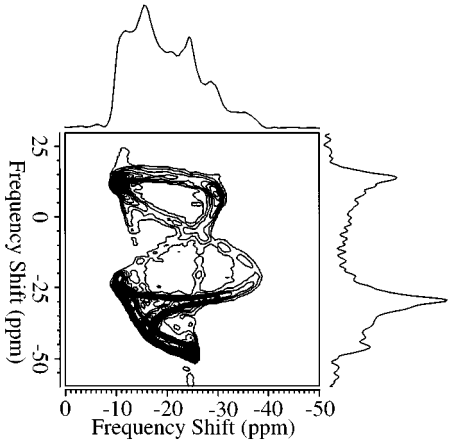

FIG. 7. Experimental two-dimensional ^{87}Rb SAS NMR spectrum and projections of Rb_2CrO_4 acquired at 11.7 T with $\theta_1=70.12°$ and $\theta_2=54.74°$. The contour levels span from 5% to 100% in 5% increments. The horizontal dimension is the ω_2 (MAS) dimension. The one-dimensional spectrum above the contour plot is a projection, a summation over ω_1, that corresponds to a MAS spectrum and is nearly identical to a MAS spectrum acquired separately. The one-dimensional spectrum to the side of the contour plot, is a projection over ω_2 and is nearly identical to a spectrum acquired separately with the sample spinning about 70.12° relative to the magnetic field.

with a MAS spectrum acquired separately, as well as with a simulation of the one-dimensional spectrum calculated using the same parameters as above. For simple systems, the quadrupolar parameters are obtainable using the SAS technique, with an accuracy equal to or greater than that obtained from one-dimensional magic-angle spinning spectra.

Many two-dimensional spectra (not shown) were calculated to determine the effects of a small anisotropic chemical shift (δ) on SAS spectra. For $I=3/2$ and a moderate C_Q (3 MHz) at a resonance frequency of 100 MHz, a δ of less than 10 ppm is difficult to detect. However, a δ of 15 ppm can cause significant changes in the spectral features. The effect of the chemical shift anisotropy on the two-dimensional line shape depends on the relative orientation of the two principle axis systems and is more significant when the two principle axis systems are not coincident, especially when V_{zz} and σ_{zz} are not parallel ($\beta\neq0°$).

Shown in Fig. 6 is a ^{87}Rb SAS NMR spectrum of Rb_2SO_4 acquired at 9.4 T; also shown separately are the spectra of the individual sites and the corresponding simulations. Rb_2SO_4 has two rubidium sites that are resolved with θ_1 equal to 90°. The spectrum was acquired with the sample spinning at the relatively fast rate of 10 kHz. Spinning sidebands are still apparent due to the large quadrupolar interactions and result in the intensity of the two sites overlapping in the one-dimensional MAS spectrum. In the SAS spectrum the signal is spread into a two-dimensional frequency domain yielding greater resolution and nearly complete separation of the two sites. The simulations of the SAS spectrum yield $C_Q=5.3$ and 2.6 MHz, $\eta_Q=0.1$ and 1.0, $\delta_{iso}=16$, and 40 ppm for the two sites, respectively. These results are consistent with those obtained by Baltisberger *et al.*[40] from field dependent DAS measurements, by Fernadez *et al.*[15] from MAS spectra, and for the $C_Q=2.6$ MHz site by Cheng *et al.*[13] from measurements of static powder samples. Cheng *et al.* reported much different values for the $C_Q=5.3$ MHz site.[13] Overlap between the two sites in the one-dimensional MAS spectrum (not shown) complicates the accurate determination of these parameters using one-dimensional techniques.

The small discrepancy between the simulated and experimental spectra shown in Fig. 6 is due to the anisotropic chemical shifts of both sites. The anisotropic chemical shifts have been reported by Fernandez *et al.* from simulations of one-dimensional MAS spectra to be 12 and 35 ppm for the $C_Q=2.6$ and 5.3 MHz sites, respectively.[15] The relative orientations of the principle axis systems were also reported, though with large uncertainties. While in some cases a better agreement between the experimental and simulated SAS spectra is obtained by including anisotropic chemical shifts, simulations incorporating the results of Fernandez *et al.*[15] do not match the experimental spectrum better than simulations neglecting the anisotropic chemical shift. Further refinements are needed to accurately determine the small anisotropic chemical shifts and the relative orientation of the principle axis systems.

In Fig. 7, the ^{87}Rb SAS NMR spectrum and projections of Rb_2CrO_4 acquired at 11.7 T with θ_1 and θ_2 equal to 70.12° and 54.74°, respectively are shown. The two-dimensional line shape results from the combination of quadrupolar and chemical shift interactions. The horizontal dimension corresponds to the MAS dimension. The projection above the

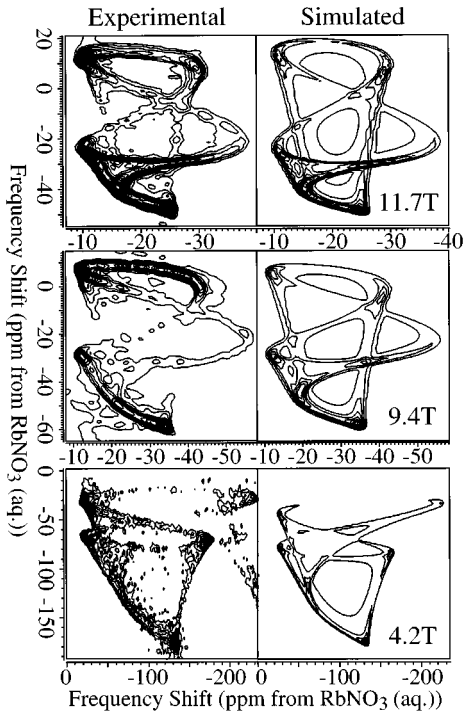

FIG. 8. Experimental and simulated two-dimensional ^{87}Rb SAS NMR spectra of Rb_2CrO_4 measured at 4.2, 9.4, and 11.7 T with $\theta_1=70.12°$ and $\theta_2=54.74°$. The same parameters were used for the simulated spectra at all three fields strengths, and are $C_Q=3.5$ MHz, $\eta_Q=0.3$, $\delta_{iso}=-7$ ppm, $\delta=-110$ ppm, $\eta_{CS}=0$, $\beta=70°$, $\gamma=0°$. The contour levels span from 5% to 100% in 5% increments. The horizontal dimension is the ω_2 (MAS) dimension.

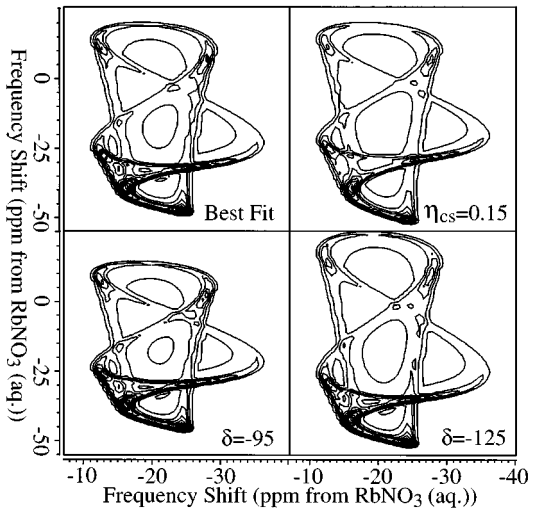

FIG. 9. Simulated two-dimensional ^{87}Rb SAS NMR spectra of Rb_2CrO_4 at 11.7 T with $\theta_1=70.12°$ and $\theta_2=54.74°$. The same parameters ($C_Q=3.5$ MHz, $\eta_Q=0.3$, $\delta_{iso}=-7$ ppm, $\delta=-110$ ppm, $\eta_{CS}=0$, $\beta=70°$, $\gamma=0°$) were used for all the simulated spectra except where noted. The contour levels span from 5% to 100% in 5% increments. The horizontal dimension is the ω_2 (MAS) dimension.

contour plot is indistinguishable from a MAS spectrum of the central transition measured independently. Both one-dimensional projections have structure; however the two-dimensional line shape contains more detail. While Rb_2CrO_4 has two rubidium sites, the site with the smaller quadrupolar interaction is selectively observed.[40] The MAS spectrum of Rb_2CrO_4 at 11.7 T has more structure than if only the quadrupolar interaction was present.[40] Both the center-band and spinning side-bands are affected by the spinning speed not being fast enough to completely average the anisotropic chemical shift. The MAS spectra of Rb_2CrO_4 at various fields were simulated using the parameters determined from the SAS experiments, and reproduce all the features in the center-band and side-bands of the experimental spectra (not shown).

In Fig. 8, the ^{87}Rb SAS NMR experimental and simulated spectra of Rb_2CrO_4, obtained with $\theta_1=70.12°$ and $\theta_2=54.74°$ acquired at 4.2, 9.4, and 11.7 T are shown. The differences among the three measured spectra reflect the dependence of the chemical shift and quadrupolar interactions on magnetic field strength. The smaller the magnetic field, the smaller the chemical shift interaction is relative to the quadrupolar interaction. Note that the spectrum acquired at the lowest field, 4.2 T, appears similar to spectra in Fig. 4 calculated considering only the quadrupolar interaction. All the simulated spectra in Fig. 8 were calculated using the following parameters, $C_Q=3.5$ MHz, $\eta_Q=0.3$, $\delta_{iso}=-7$ ppm, $\delta=-110$ ppm, $\eta_{CS}=0$, $\beta=70°$, $\gamma=0°$. α is undefined because in this case the chemical shift interaction is axially symmetric ($\eta_{CS}=0$). The fact that the same parameters fit the spectra acquired at three field strengths rigorously demonstrates the precision of the technique. The quadrupolar coupling constant, quadrupolar asymmetry parameter, and isotropic chemical shift are all consistent with the values determined using field dependent DAS measurements by Baltisberger *et al.*[40]

To determine the sensitivity of the spectra to the chemical shift parameters, spectra were calculated with δ and η_{CS} varied separately by ± 15 ppm and from 0 to 0.15, respectively, with all the remaining parameters identical to those used for the simulations shown in Fig. 8. From simulated spectra such as those presented in Fig. 9, the uncertainty in δ and η_{CS} is determined to be ± 15 ppm and less than 0.15, respectively. To determine the sensitivity of the simulated spectra on β, γ, and η_Q the spectra presented in Fig. 10 were calculated with parameters identical to those in Fig. 8 except that β, γ, and η_Q were varied separately by $\pm 5°$, from 0 to 15°, and ± 0.1, respectively. The simulated spectra calculated with γ equal to $+15°$ or $-15°$ are equivalent. From simulations such as those shown in Fig. 10, conservative error estimates for β, γ, and η_Q are $\pm 5°$, $\pm 15°$, and ± 0.1, respectively. Considering the greater accuracy in determining β compared to γ, and similar results reported by Fernandez *et al.*[15] one might suspect that this is a general trend. Further experiments on other systems can be performed to clarify this point.

Thus, the chemical shift and quadrupolar interaction parameters and the relative orientation between the principle axis systems are determined with the following accuracy: $C_Q=3.5\pm 0.2$ MHz, $\eta_Q=0.3\pm 0.1$, $\delta_{iso}=-7$ ppm, $\delta=-110\pm 15$ ppm, $\eta_{CS}=0+0.15$, $\beta=70°\pm 5°$, $\gamma=0°\pm 15°$,

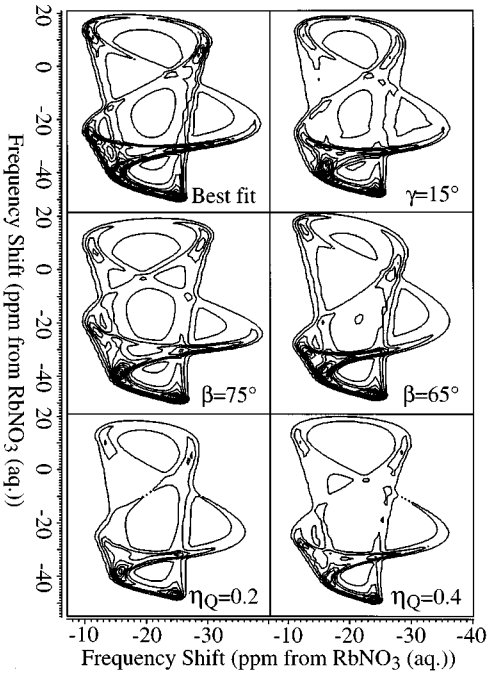

FIG. 10. Simulated two-dimensional ^{87}Rb SAS NMR spectra of Rb_2CrO_4 at 11.7 T with $\theta_1=70.12°$ and $\theta_2=54.74°$. The same parameters were used for all the simulated spectra except where noted, and are $C_Q=3.5$ MHz, $\eta_Q=0.3$, $\delta_{iso}=-7$ ppm, $\delta=-110$ ppm, $\eta_{CS}=0$, $\beta=70°$, $\gamma=0°$. The contour levels span from 5% to 100% in 5% increments. The horizontal dimension is the ω_2 (MAS) dimension.

with α undefined. These results differ significantly from those determined from one-dimensional NMR spectra of powder samples reported by Cheng *et al.*[13]

CONCLUSIONS

NMR has the potential to characterize the local atomic environment in materials and can be used to determine structure property relationships, location and distribution of substitution species, and motion and diffusion of atoms, as well as other technologically important properties in inorganic solids. With NMR, an experimentalist has the unprecedented advantage of being able to manipulate the Hamiltonian of the system under study using radio frequency pulses and sample spinning, among other techniques. The combination of these methods with multidimensional NMR techniques enables the direct correlation and/or deconvolution of multiple interactions. These ideas have been used in this paper to correlate the quadrupolar and chemical shift interactions and to determine the quadrupolar and chemical shift tensor elements, as well as the relative orientation between the two principal axis systems for a rubidium site in Rb_2CrO_4.

The technique and formalizms described in this paper can also be applied to correlate quadrupolar and dipolar interactions, which would enable the assignment of the quadrupolar tensor to the molecular frame defined by the internuclear axes. The ability to correlate the quadrupolar interaction with either the chemical shift or dipolar interactions greatly increases the amount of information obtainable using NMR and will lead to a better understanding of the quadrupolar and chemical shift interactions. It is anticipated that through empirical relations and comparison with *ab initio* calculations a better comprehension of materials on an atomic level basis will also be achieved.

Extension of these methods to a three-dimensional experiment by incorporating a purely isotropic dimension is currently under way and will be applicable to systems with multiple atomic sites and those with a distribution of isotropic shifts such as glasses.

ACKNOWLEDGMENTS

This work was supported by the Director, Office of Energy Research, Office of Basic Energy Sciences, Materials Sciences Division of the U.S. Department of Energy under Contract No. DE-AC03-76SF00098. This work was presented in part at the 36th Experimental Nuclear Magnetic Resonance Conference, Boston, MA, March 1995; Abstract P347.

[1] A. Samoson, E. Lippmaa, and A. Pines, Mol. Phys. **65**, 1013 (1988).
[2] A. Llor and J. Virlet, Chem. Phys. Lett. **152**, 248 (1988).
[3] L. Frydman and J. S. Harwood, J. Am. Chem. Soc. **117**, 5367 (1995).
[4] I. Farnan, P. J. Grandinetti, J. H. Baltisberger, J. F. Stebbins, U. Werner, M. A. Eastman, and A. Pines, Nature **358**, 31 (1992).
[5] P. J. Grandinetti, J. H. Baltisberger, I. Farnan, J. F. Stebbins, U. Werner, and A. Pines, J. Phys. Chem. **99**, 12341 (1995).
[6] K. Narita, J. Umeda, and H. Kusumoto, J. Chem. Phys. **44**, 2719 (1966).
[7] I. J. Lowe, Phys. Rev. Lett. **2**, 285 (1959).
[8] E. R. Andrew, A. Bradbury, and R. G. Eades, Nature **182**, 1659 (1958).
[9] E. R. Andrew, A. Bradbury, and R. G. Eades, Nature **183**, 1802 (1959).
[10] S. Ganapathy, S. Schramm, and E. Oldfield, J. Chem. Phys. **77**, 4360 (1982).
[11] F. Lefebvre, J. P. Amoureux, C. Fernandez, and E. G. Derouane, J. Chem. Phys. **86**, 6070 (1987).
[12] P. J. Chu and B. C. Gerstein, J. Chem. Phys. **91**, 2081 (1989).
[13] J. T. Cheng, J. C. Edwards, and P. D. Ellis, J. Phys. Chem. **94**, 553 (1990).
[14] P. W. France, J. Magn. Reson. **92**, 30 (1991).
[15] C. Fernandez, J. P. Amoureux, and P. Bodart, J. Magn. Reson. Series a **113**, 205 (1995).
[16] J. Hirschinger, T. Mongrelet, C. Marichal, P. Granger, J. M. Savariault, E. Deramond, and J. Galy, J. Phys. Chem. **97**, 10301 (1993).
[17] W. P. Power, R. E. Wasylishen, S. Mooibroek, B. A. Pettitt, and W. Danchura, J. Phys. Chem. **94**, 591 (1990).
[18] C. Fernandez, P. Bodart, and J. P. Amoureux, Solid State Nucl. Magn. Reson. **3**, 79 (1994).
[19] J. Skibsted, N. C. Nielsen, H. Bildsoe, and H. J. Jakobsen, J. Am. Chem. Soc. **115**, 7351 (1993).
[20] H. J. Jakobsen, J. Skibsted, H. Bildsøe, and N. C. Nielsen, J. Magn. Reson. **85**, 173 (1989).
[21] R. K. Hester, J. L. Ackermann, B. L. Neff, and J. S. Waugh, Phys. Rev. Lett. **36**, 1081 (1976).
[22] E. F. Rybaczewski, B. L. Neff, J. S. Waugh, and J. S. Sherfinski, J. Chem. Phys. **67**, 1231 (1977).
[23] J. S. Waugh, Proc. Natl. Acad. Sci. USA **73**, 1394 (1976).
[24] M. A. Eastman, P. J. Grandinetti, Y. K. Lee, and A. Pines, J. Magn. Reson. **98**, 333 (1992).
[25] K. T. Mueller, G. C. Chingas, and A. Pines, Rev. Sci. Instrum. **62**, 1445 (1991).
[26] G. Drobny, A. Pines, S. Sinton, D. P. Weitekamp, and D. Wemmer, Faraday Symp. Chem. Soc. **13**, 49 (1979).
[27] D. J. States, R. A. Haberkorn, and D. J. Ruben, J. Magn. Reson. **48**, 286 (1982).
[28] J. H. Baltisberger, Ph.D. thesis, University of California, 1993.
[29] U. Haeberlen, *High Resolution NMR in Solids: Selective Averaging, Advances in Magnetic Resonance, Supplement 1* (Academic, New York, 1976).

[30] M. Mehring, *High Resolution NMR in Solids* (Springer, New York, 1983).
[31] A. R. Edmonds, *Angular Momentum in Quantum Mechanics* (Princeton University Press, Princeton, NJ, 1960).
[32] M. E. Rose, *Elementary Theory of Angular Momentum* (Wiley, New York, NY, 1957).
[33] D. W. Alderman, M. S. Solum, and D. M. Grant, J. Chem. Phys. **84**, 3717 (1986).
[34] A. Bax, N. M. Szeverenyi, and G. E. Maciel, J. Magn. Reson. **55**, 494 (1983).
[35] T. Terao, T. Fujii, T. Onodera, and A. Saika, Chem. Phys. Lett. **107**, 145 (1984).
[36] A. Medek, J. H. Sachleben, and L. Frydman, Presented at the 36th Experimental Nuclear Magnetic Resonance Conference, Boston, Massachusetts, March 1995, p. 377.
[37] A. Medek, J. H. Sachleben, P. Beverwyk, and L. Frydman, J. Chem. Phys. **104**, 5374 (1996).
[38] L. Frydman, G. C. Chingas, Y. K. Lee, P. J. Grandinetti, M. A. Eastman, G. A. Barrall, and A. Pines, J. Chem. Phys. **97**, 4800 (1992).
[39] J. P. Amoureux, C. Fernandez, and F. Lefebvre, Magn. Reson. Chem. **28**, 5 (1990).
[40] J. H. Baltisberger, S. L. Gann, E. W. Wooten, T. H. Chang, K. T. Mueller, and A. Pines, J. Am. Chem. Soc. **114**, 7489 (1992).